



HAL
open science

Magnetic field effect on the dielectric constant of glasses: Evidence of disorder within tunneling barriers

J Le Cochee, F Ladieu, P Pari

► To cite this version:

J Le Cochee, F Ladieu, P Pari. Magnetic field effect on the dielectric constant of glasses: Evidence of disorder within tunneling barriers. *Physical Review B: Condensed Matter and Materials Physics* (1998-2015), 2002, 66, 10.1103/PhysRevB.66.064203 . cea-01395460

HAL Id: cea-01395460

<https://cea.hal.science/cea-01395460>

Submitted on 10 Nov 2016

HAL is a multi-disciplinary open access archive for the deposit and dissemination of scientific research documents, whether they are published or not. The documents may come from teaching and research institutions in France or abroad, or from public or private research centers.

L'archive ouverte pluridisciplinaire **HAL**, est destinée au dépôt et à la diffusion de documents scientifiques de niveau recherche, publiés ou non, émanant des établissements d'enseignement et de recherche français ou étrangers, des laboratoires publics ou privés.

Magnetic field effect on the dielectric constant of glasses : an evidence of disorder within tunneling barriers ?

J. Le Cocheq,¹ F. Ladieu,^{1,*} and P. Pari²

¹DSM/DRECAM/LPS, C.E.Saclay, 91191 Gif sur Yvette Cedex, France

²DSM/DRECAM/SPEC, C.E.Saclay, 91191 Gif sur Yvette Cedex, France

(Dated: August 12, 2013)

The magnetic field dependence of the low frequency dielectric constant $\epsilon_r(H)$ of a structural glass $a - \text{SiO}_{2+x}\text{C}_y\text{H}_z$ was studied from 400 mK to 50 mK and for H up to 3 T. Measurement of *both* the real and the imaginary parts of ϵ_r is used to eliminate the difficult question of keeping constant the temperature of the sample while increasing H : a non-zero $\epsilon_r(H)$ dependence is reported in the same range as that one very recently reported on multicomponent glasses. *In addition* to the recently proposed explanation based on interactions, the reported $\epsilon_r(H)$ is interpreted quantitatively as a consequence of *the disorder* lying within the nanometric barriers of the elementary tunneling systems of the glass.

PACS numbers: 61.43.Fs, 77.22.Gm, 72.20.Ht, 72.20.My

I. INTRODUCTION

Since the seventies [1], it is well established that at low temperature T , the properties of amorphous solids differ strongly from their crystalline counterparts. This is currently explained [2] within the tunneling two-level system (TLS) model, stating that the only relevant degrees of freedom at low T are particles going back and forth between two neighboring sites of equilibrium. Indeed, the TLS model accounts for various properties of glasses below ~ 1 K. A closer look, however, reveals that the TLS model often does not quantitatively account for the measured quantities. Since the late eighties, considerable efforts have been made to include interactions between TLS's in order to explain such discrepancies [3] and justify the TLS model from first principles [4], [5] or, at least, to give a more consistent picture of TLS's [6], [7]. However, the lack of TLS microscopic information allowed to consider interactions either to be weak [5] or strong [6], [7], [8] : these opposite starting points echo Leggett and Yu's question : "Is there anything really tunneling in glasses ?" [9].

The purpose of this work is to gain some microscopic information on TLS's by studying the magnetic field effect on a glassy property, namely the 1 kHz dielectric constant ϵ_r . Indeed, for a charge Q , the tunneling transparency of a barrier of size a is strongly modified by magnetic fields H of the order of $H_c = \frac{\hbar}{Qa^2}$: this is due to the (H dependent) difference of quantum phase picked up by the various paths under the barrier [7]. However, setting the usual TLS parameters, $a \simeq 0.2$ nm and $Q = e$, with e the electronic charge, leads to $H_c \simeq 10^4$ T, a value so large that it seemed to explain Frossati *et al*'s results [10] reporting no detectable H effects on ϵ_r . Recently, however, detectable $\epsilon_r(H)$ effects were reported below 80

mK (and down to 1 mK) on a multicomponent glass [8], [11]. Very strikingly, $\epsilon_r(H)$ is peaked around $H_c \simeq 0.03$ T, a very low value accounted for by using interactions : at low T , it was argued that interactions correlate a large number $N \gg 1$ of TLS's and that the resulting spectrum resembles that of a single TLS with a charge $Q = Ne$ (and a renormalized tunneling energy Δ_0). In this work, a detectable $\epsilon_r(H)$ effect is reported on a $a - \text{SiO}_{2+x}\text{C}_y\text{H}_z$ glass for $50 \text{ mK} \leq T \leq 400 \text{ mK}$ and H up to 3 T. Even if our glass is not really a model glass (such as the various forms of vitreous silica, e.g. Suprasil), the $\epsilon_r(H)$ dependence reported here shows that these effects are not restricted to the multicomponent glass studied previously [8], [11], favoring the idea that such effects are general in structural glasses. Furthermore our work shows, as stated previously [12], that such measurements demand special experimental care since $\epsilon_r(H)$ effects are quite small: $\delta\epsilon'_r(H)/\epsilon'_r$ lies typically in the $10^{-6} - 10^{-5}$ range (ϵ'_r is the real part of ϵ_r). This is why, after a brief description of the experimental setup, it is explained how to overcome the difficult question of keeping T constant with great accuracy, while increasing H . The resulting $\epsilon'_r(H)$ effect is then accounted for by using numerical calculations of the H effect on the tunneling transparency of a *disordered* nanometric barrier. As explained below, this additional mechanism should not contradict the one based upon interactions.

II. EXPERIMENTAL SETUP

The sample was deposited on a $a - \text{SiO}_2$ substrate as follows: i) a $0.1 \mu\text{m}$ thick Cu layer was first evaporated, ii) a $L = 0.8 \mu\text{m}$ thick $a - \text{SiO}_{2+x}\text{C}_y\text{H}_z$ layer was then deposited by a 13 MHz plasma vapor technique using TetraEthylOrthoSilane mixed with He [13] iii) a $0.08 \mu\text{m}$ thick Cu layer, followed by a $0.04 \mu\text{m}$ Au layer was evaporated. Both electrodes are 3 mm large 10 mm long ribbons recovering each other along $\simeq 3$ mm

*ladieu@drecam.cea.fr

(i.e., the capacitance surface is $S \simeq 9 \text{ mm}^2$) : the opposite ends of the electrodes are free of glass deposit allowing an ohmic contact to be made with a Cu wire glued with Ag paste. These two Cu wires are soldered to the inner wires of cryogenic coaxial cables going from room temperature to the cold copper box embedding the sample : this box is related to the mixing chamber of the dilution fridge by a thermal impedance and contains a RuO_2 resistive thermometer whose resistance will be called θ_{RuO_2} throughout this work (to avoid any confusion with the parallel resistance R of the glass sample). The sample substrate was glued with varnish on a copper sample holder for thermalization. To decrease possible H -dependent heating in the electrodes, H was set parallel to the electrodes (i.e., perpendicular to the 1 kHz measuring field \mathcal{E}). Semi-rigid home-made coaxial cables were installed at the top of the fridge and directly plugged in the Andeen-2500A capacitance bridge. The capacitance bridge was used in its parallel option, yielding $C \propto \epsilon'_r$ and $G \propto \epsilon''_r$, but throughout this work it was chosen to report on C and $R = 1/G$ due to the great similarity of the $C(T)$ and $R(T)$ curves (see Fig. 1) : this strongly confirms that the reported R at low T is not some parasitic edge effect but has the same origin that the reported C , namely the TLS's.

From 300 K to 4.2 K, the capacitance C typically halves, while the parallel resistance R increases by a factor $\simeq 100$. Below 4.2 K, C decreases, reaches its minimum for $T_{rev.}$ and then increases below $T_{rev.}$ before reaching a ultra low T saturation value $C_{sat.}$. According to the standard TLS model the C decrease above $T_{rev.}$ is due to progressive freezing of the diagonal (or relaxational) part of the response, while the C increase below $T_{rev.}$ comes from the induced off-diagonal (or resonant) part of the susceptibility : this effect enlarges as T decreases as do all quantum effects.

III. OBTAINING $\delta\epsilon'_r(H)$

A. Proof that a non-zero $\delta\epsilon'_r(H)$ exists

Figure 1 shows $C(T)$ and $R(T)$ curves when a 1 kHz field $\mathcal{E} = 3V/0.8 \mu\text{m} = 3.75 \text{ MV/m}$ is used. The high value of $T_{rev.} \simeq 0.3 \text{ K} \simeq 8T_{rev.}(\mathcal{E} \rightarrow 0)$ reveals that such fields correspond to the strongly nonlinear regime [14]. Such large fields were used with a large integration time (100 s) so as to reduce the bridge uncertainties c_{noise} (resp. r_{noise}) over C (resp. R) measurements down to $c_{noise}/C = \pm 10^{-7}$ (resp. $r_{noise}/R = \pm 10^{-5}$). Large fields were also used in [11].

The second key point to investigate small $\epsilon_r(H)$ effects is to be able to increase H while keeping T accurately constant. It demands either to set up a H -independent thermometry, which is extremely difficult over an extended T range (it may have been the way used in [8], [11]); or, at least, to correct T of the magnetoresistance of the thermometer. However, such a correction cannot be

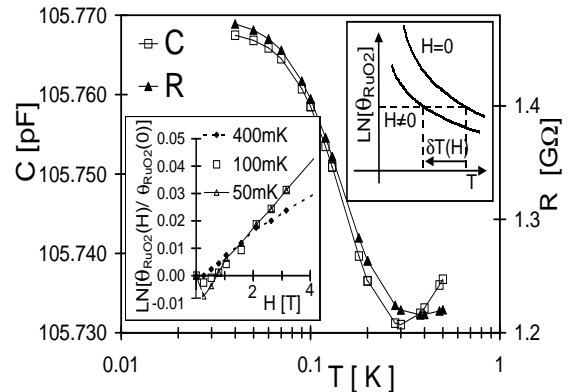


FIG. 1: $C(T)$ (left axis) and $R(T)$ (right axis) when a 1 kHz measuring field $\mathcal{E} = 3.75 \text{ MV/m}$ is applied to the glass sample. *Lower inset*: $\theta_{\text{RuO}_2}(H)$ dependence measured assuming that the $\mathcal{P}(T)$ relationship does not depend on H (see text). *Upper inset*: Schematic effect of a negative RuO_2 magnetoresistance : increasing H while keeping θ_{RuO_2} constant leads to a small decrease of T , i.e., $\delta T(H) < 0$.

done with great accuracy since the standard technique for measuring the $\theta_{\text{RuO}_2}(H)$ dependence is as follows [17] : *i*) For $H = 0$ the relationship between the power \mathcal{P} injected in the fridge and the resulting T is first recorded ; *ii*) For a given \mathcal{P} , H is slowly raised to a given value, and the measured $\theta_{\text{RuO}_2}(H) - \theta_{\text{RuO}_2}(0)$ at thermal equilibrium is attributed to the magnetoresistance of the thermometer : the corresponding results are shown in the lower inset of Fig. 1 and lead to corrections of the order of 2 – 5% on T when H is raised up to a few T. However, these $\theta_{\text{RuO}_2}(H)$ measurements lie on the key assumption that the $\mathcal{P}(T)$ relationship does not depend at all on H : this cannot hold accurately, e.g., due to the dissipation of energy resulting from the vibrations of the fridge within the magnetic field. These small and complicated effects cannot be ignored when seeking small $\epsilon_r(H)$ effects which, translated into a thermal equivalent, amount to an effective variation of T lying in the 0.1 – 5% range (see **B**)2) below).

Going back to the C, R measurements, the fact that both $\mathcal{P}(T)$ and $\theta_{\text{RuO}_2}(T)$ relationships slightly depend on H implies that T cannot be made accurately constant when H is increased. For practical reasons, the $C(H), R(H)$ measurements were made letting \mathcal{P} automatically adjust so as to keep the θ_{RuO_2} value fixed at any H value : raising H while keeping θ_{RuO_2} constant leads to a small shift $\delta T(H)$ of the temperature of the experiment as depicted in the upper inset of Fig. 1.

The measured variations $\delta C(H) = [C(H) - C(0)]_{\text{constant } \theta_{\text{RuO}_2}}$ are displayed in Fig. 2 for various T values measured at $H = 0$. The key point is that the

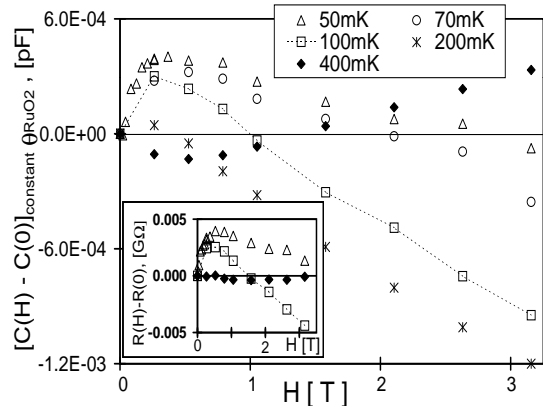


FIG. 2: $\delta C(H)$ measured by keeping θ_{RuO_2} constant while increasing H (the various T labeling the curves are at $H = 0$). *Inset*: Corresponding data for $\delta R(H)$ (same symbols). The fact that $\delta R(H)$ and $\delta C(H)$ do not vanish at the same H cannot be explained by using *only* $\delta T(H)$ effects but implies that a $\delta\epsilon_r(H)$ dependence exists in the sample. The error bars $c_{\text{noise}} = \pm 10^{-5}$ pF and $r_{\text{noise}} = \pm 10^{-5}$ G Ω are much smaller than the data symbols.

$\delta T(H)$ dependence cannot explain all the qualitative features of Fig. 2. For example, whatever $\delta T(H)$ may be, if $\delta\epsilon_r(H)$ were zero, $\delta C(H)$ and $\delta R(H)$ would vanish at the same H : this is clearly contradicted by the 50 mK, 100 mK and 400 mK data reported on Fig. 2. *This proves that a $\epsilon_r(H)$ dependence exists in our sample* but that an accurate correction of the $\delta T(H)$ effects must be done on the data of Fig. 2. This correction cannot be done with the data of the inset of Fig. 1 since, as above evoked, the sought $\epsilon_r(H)$ is smaller than the accuracy of the $\delta T(H)$ estimate.

B. Obtaining the order of magnitude of $\delta\epsilon_r'(H)$

At this step, the existence of a detectable $\delta\epsilon_r'(H)$ dependence is established but an accurate suppression of $\delta T(H)$ effects is still missing. It is shown here that using *both* $\delta R(H)$ and $\delta C(H)$ allows to draw from Fig. 2 the order of magnitude of $\delta\epsilon_r'(H)$, i.e., to know its value within a scale factor $0.1 < \eta < 10$ (see Eq. (2) below): this interval might seem to be very large, but we will see in the next section that the physical interpretation only involves $\ln(\eta)$.

1. Overview of the method

The key idea is that since the relative variations of all the involved quantities are small, first order expan-

sions are accurate. Defining $\delta X(H) = X(H) - X(0)$ for any quantity X measured as a function of H keeping the θ_{RuO_2} value constant, one gets :

$$\delta C(H) = \left(\frac{\partial C}{\partial T} \right) \delta T(H) + \delta C_{\text{int.}}(H), \quad (1a)$$

where the measured $\delta C(H)$ is shown on Fig. 2, $\delta C_{\text{int.}}(H)$ is proportionnal to the sought intrinsic variation of $\delta\epsilon_r'(H)$ and throughout this work, all the partial derivatives with respect to T are taken at $H = 0$. Introducing the corresponding quantity $\delta R_{\text{int.}}(H)$, an equation similar to Eq. (1a) is obtained for R measurements.

$$\delta R(H) = \left(\frac{\partial R}{\partial T} \right) \delta T(H) + \delta R_{\text{int.}}(H). \quad (1b)$$

Combining Eqs. (1a) and (1b) allows to *accurately* eliminate $\delta T(H)$, and to get :

$$\delta C_{\text{int.}}(H) = \eta \left(\frac{\left(\frac{\partial C}{\partial T} \right)}{\left(\frac{\partial R}{\partial T} \right)} \delta R(H) - \delta C(H) \right), \quad (2a)$$

with $\eta = \frac{1}{(\alpha-1)}$ and α is defined by :

$$\alpha = \frac{\delta R_{\text{int.}}(H)}{\delta C_{\text{int.}}(H)} \frac{\left(\frac{\partial C}{\partial T} \right)}{\left(\frac{\partial R}{\partial T} \right)}. \quad (2b)$$

α is introduced here as an attempt to eliminate one of the three unknown quantities among $\delta T(H)$, $\delta C_{\text{int.}}(H)$ and $\delta R_{\text{int.}}(H)$ since only two quantities, $\delta C(H)$ and $\delta R(H)$, are measured. α cannot be predicted since, for strong \mathcal{E} , a comprehensive treatment of the TLS dynamics, including quantum coherence effects, is still missing : at present, even the $C(T)$ curve is not well accounted for [14]. However, within the framework of the standard TLS model, α and η *cannot depend on H* since, as we show below, $\Delta_{0,\text{max}}$ is the only parameter of the TLS model which might slightly depend on H : neglecting, as above, any second order terms, both the real and the imaginary parts of $\delta\epsilon_r(H)$ (i.e., both $\delta C_{\text{int.}}(H)$ and $\delta R_{\text{int.}}(H)$) are expected to be proportionnal to the *same* small $\delta\Delta_{0,\text{max}}(H)/\Delta_{0,\text{max}}$ (see Eq. (4)).

There is no similar argument stating that, generally, α and $\eta = 1/(\alpha-1)$ cannot depend on T . It is shown in the section A of the Appendix, by using the shape of the curves of Fig. 2 and quite general arguments, that η lies, *at any reported T* , in $[0.1, 10]$, an interval which will turn out to be "small" enough to neglect any $\eta(T)$ variations (see section IV). Basically, it is shown in the Appendix that the $\delta T(H)$ influence on the measured $\delta C(H)$ and $\delta R(H)$ enlarges as H is increased : the quasilinear decrease of $\delta C(H)$, $\delta R(H)$ seen in Fig. 2 at large H thus comes from $\delta T(H)$ effects (at 400 mK it turns to a quasilinear increase due to the fact that $\partial C/\partial T > 0$ contrarily to the case of lower T data).

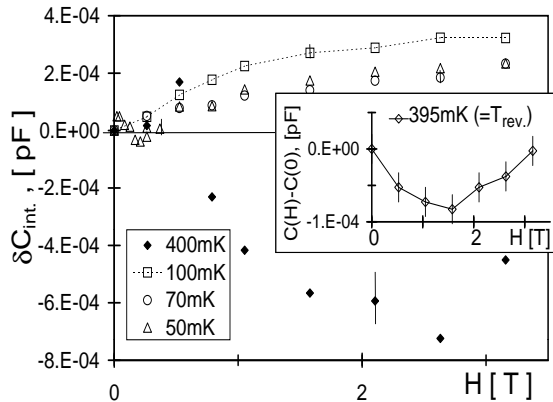


FIG. 3: $\delta C_{int.}(H) \propto \delta \epsilon'_r$ drawn from Fig. 2 data by using Eq. (2a) with $\eta = 1$. For clarity the error bar (see Eq. (3)) is reported only for one H at each T : it is much stronger at 400 mK than below 100 mK where error bars hardly exceed the size of the data symbols. *Inset*: $\delta C(H)$ measured just at $T_{rev.}$ (with a larger field $\mathcal{E} = 8.75$ MV/m to further increase the signal to noise ratio): due to the $\partial C/\partial T = 0$ at $T_{rev.}$ the use of Eq. (2a) is not necessary at low H (at higher H , $\delta T(H)$ is no longer negligible and produces the $\delta C(H)$ increase). Comparison of the data at $T_{rev.}$ to those at 400 mK supports the idea that $\eta > 0$ at 400 mK.

2. The most salient features of $\delta C_{int.}(H)$

Since $0.1 < \eta < 10$, the order of magnitude of $\delta C_{int.}(H)$ is obtained by setting $\eta = 1$ and disregarding any possible $\eta(T)$ variations within this interval: the resulting transformation of the data of Fig. 2 through Eq. (2a) is shown on Fig. 3. $\delta C_{int.}(H)$ is positive for the lowest temperatures (except for three low fields at 50 mK, see below) and negative at higher T , i.e., in the vicinity of $T_{rev.}$.

The 200 mK data were not reported on Fig. 3 since they lie very close to zero. Indeed, it seemed more important to report, in the inset of Fig. 3, on $\delta C(H)$ measured just at $T_{rev.}$ (measured with a larger field $\mathcal{E} = 8.75$ MV/m to further increase the signal to noise ratio). For the inset of Fig. 3, at low H , the $\delta T(H)$ contribution (see Eq. (1a)) to $\delta C(H)$ is negligible since $\partial C/\partial T = 0$ just at $T_{rev.}$ (at large H this is no longer true due to the increase of $\delta T(H)$, yielding the quasilinear increase of $\delta C(H)$). The important point here is the decrease of $\delta C(H, T_{rev.})$ at low H : it further confirms that $\delta C_{int.}(H)$ is negative in the vicinity of $T_{rev.}$ and that $\eta > 0$ at 400 mK. Note that the results of Fig. 3 were reproduced on a second similar sample.

Let us translate the data of Fig. 3 to a thermal equivalent by using $\delta T_{int.C} = \delta C_{int.}(H)/(\frac{\partial C}{\partial T})$ (remember that $\delta C_{int.}(H)$ are calculated by setting $\eta = 1$): it is found that $\delta T_{int.C}(H)$ reaches at most 7% of T at 50 mK, 2%

at 70 mK, 1% at 100 mK and 4% at 400 mK. *Beyond chemical differences between glasses, this might explain why, with an uncertainty on T of $\pm 5\%$, previous studies reported undetectable $\epsilon_r(H)$ effects [10].* Adding quadratically the uncertainties on both terms of the right hand-side of Eq. (2a), the final uncertainty c_{err} about the $\delta C_{int.}(H)$ reported on Fig. 3 reads :

$$c_{err} = \eta \sqrt{(c_{noise})^2 + (r_{noise} \frac{\partial C}{\partial T})^2 (\frac{\partial R}{\partial T})^{-2}}. \quad (3)$$

On Fig. 3, c_{err} was reported for each T : due to the strong decrease of $\partial R/\partial T$, it is much stronger at 0.4 K than at low T where it hardly exceeds the symbol size. However, even at 0.4 K, c_{err} amounts to an uncertainty over T of $\pm 0.5\%$, ten times smaller than in [10].

Let us note that $\delta C_{int.}(H)/c_{err}$ does not depend on the chosen $\eta = 1$: the trends of $\delta C_{int.}(H)$ reported on Fig. 3 are thus reliable at each T , even if the possible $\eta(T)$ dependence forbids any accurate comparison of $\delta C_{int.}(H)$ at different T . Comparing Fig. 3 with Strehlow's results [11], our $\delta \epsilon'_r(H)$ is somewhat smaller but lies in the same range. As in [11], our $\delta \epsilon'_r(H)$ *might* be peaked around $H \simeq 0.02$ T for our lowest T , but this effect is too close to our c_{err} to be systematically studied.

IV. PHYSICAL INTERPRETATION

Let us move to the interpretation of Fig. 3. First, note that, due to the T -dependence of the data of Fig. 2 and Fig. 3, the reported $\delta \epsilon'_r(H)$ can be attributed neither to the coaxial cables nor to the "matrix" surrounding TLS's. Furthermore, the change of sign of $\delta C_{int.}(H)$ in the vicinity of $T_{rev.}$ excludes a role of the electrode-glass interfaces and further confirms that TLS's are responsible for the reported $\delta \epsilon'_r(H)$. Last, it is shown in the section B of the Appendix that spin effects, if any, can be ruled out at low enough T , i.e., well below $T_{rev.}$: this is why we will focus on the positive $\delta \epsilon'_r(H)$ observed at $T \leq 200$ mK.

A. Going from $\delta C_{int.}(H)$ to $\delta \Delta_{0,max}(H)$

For the part of the capacitance C_{TLS} coming from TLS's, the usual result [14] below $T_{rev.}$ can thus be used: $C_{TLS} = \mathcal{C} \ln(E_{max}/k_B T)$ where k_B is Boltzmann constant, $E_{max} = \sqrt{\Delta_{max}^2 + \Delta_{0,max}^2}$ is the maximum inter-level spacing of TLS's, and the constant $\mathcal{C} \simeq 0.03$ pF is determined by fitting the increase of $C(T)$ of Fig. 1 below $T_{rev.}$ (details are given below).

Since both Δ (see section B of the Appendix) and \mathcal{C} [16] are H -independent, *the reported $\delta \epsilon'_r(H)$ is interpreted as a $\Delta_{0,max}(H)$ dependence, yielding :*

$$\frac{2\delta C_{int.}(H)}{\mathcal{C}} = \frac{\delta\Delta_{0,max}(H)}{\Delta_{0,max}(0)} = \ln\left(\frac{\Delta_{0,max}(H)}{\Delta_{0,max}(0)}\right), \quad (4)$$

where the standard assumption $\Delta_{max} = \Delta_{0,max}$ is responsible for the factor 2 in the left hand-side of Eq. (4).

Let us note that the expression of C_{TLS} used to derive Eq. (4) only holds accurately between 90 mK and 200 mK since, at lower T , the $C(T)$ curve tends to saturate. This failure of the fit at low T is due to the fact that the above expression of C_{TLS} is well established only in the linear regime, and that a comprehensive treatment for the strong \mathcal{E} used here is still missing. However, this formula should capture the essential part of the physics since it expresses that, well below $T_{rev.}$, the TLS susceptibility is due to the quantum transitions coherently induced by \mathcal{E} . Since, physically, it is likely that tunneling plays a key role in the nonlinear C_{TLS} at low T , Eq. (4) should finally hold, up to a multiplicative prefactor which can be disregarded just like η (see below).

B. A possible microscopic explanation of

$$\delta\Delta_{0,max}(H)$$

A $\Delta_{0,max}(H)$ dependence means that the tunnel transparency is affected by H . This is well known in another kind of disordered insulators, namely Anderson insulators (e.g. lightly doped semiconductors) where electronic states are localized due to potential disorder. At very low frequency, transport in Anderson insulators occurs by hopping on a fractal percolating path strongly affected by H . H effects are smaller at high frequencies where the conducting path is broken since only the fastest hops contribute: note that, since they are disconnected from each other, each of these fast back-and-forth hops is a TLS. In both limits, H effects were accounted for [17], [18] by studying the tunnel transparency Δ_0 between two sites separated by a disordered barrier depicted in the inset of Fig. 4: tunneling between the two sites of the (quasisymmetric) TLS separated by the distance a is strongly affected by the potential disorder coming from the structural disorder within the tunneling barrier itself. This is modeled by a three dimensional network of "impurities" (whose unit length is the elastic mean free path λ_{el}) and Δ_0 results from the coherent sum of all quantum paths along the impurity network: at $H = 0$, a path picks up a phase -1 each time it diffuses on an impurity whose energy e_i is smaller than that of the TLS. Since the e_i are drawn at random, Δ_0 must be first averaged over disorder (noted hereafter with $\langle \rangle$).

Using this model to account for the measured $\delta\epsilon'_r(H)$ is obviously an oversimplification. Indeed, TLS's might be more complicated than a *unique* charge going back and forth between two sites separated by a : a TLS could be a group of charges, a 'molecule', and more generally any charged species with two spatially separated potential minima. However, we show now that this model ac-

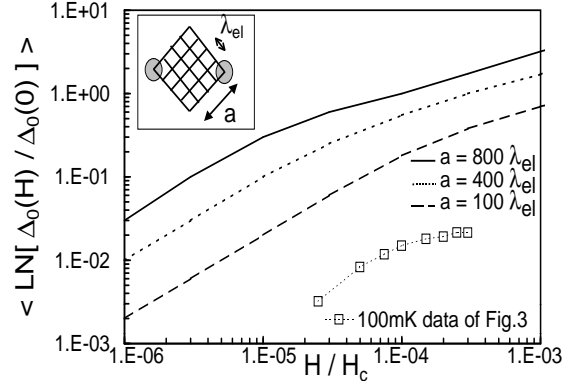


FIG. 4: *Inset*: Schematic view of the disorder lying within the tunnel barrier of size $\sim a$ between the two sites (gray circles) of a TLS: the potential fluctuations are modeled by a set of "impurities" of interspacing λ_{el} whose energies are drawn at random either well above or well below that of the TLS. *Main figure*: Δ_0 results from the coherent sum of all the paths linking the TLS sites: due to the additional quantum phase introduced by H for each path, $\langle \ln \Delta_0 \rangle$ increases with H , the H^2 dependence at very low H (unreported) turning continuously to a $H^{0.5}$ behavior at higher fields (ensemble averaging over the possible "impurities" configurations is indicated by $\langle \rangle$ and $Hc = \frac{\hbar}{e\lambda_{el}^2}$). The three curves for $a/\lambda_{el} \geq 100$ are calculations drawn from Medina *et al*'s work [19] and the 100 mK data of Fig. 3 are reported by using Eq. (4). Both the sign and the sublinear behavior of our data are well accounted for by the calculations. Extrapolation from the logarithmic behavior at large a/λ_{el} gives $a/\lambda_{el} \simeq 5 - 10$ for our sample, yielding an elementary dipole $p_0 \sim 10$ D not that far from the one drawn from echo measurements.

counts for most of the salient features of the low- T $\delta\epsilon'_r(H)$ reported in Fig. 3.

C. Accounting for the data by using the disordered tunneling barrier model

Figure 4 is drawn from Medina *et al*'s calculations [19] and shows that $\langle \ln \Delta_0 \rangle$ increases with H (in Fig. 4 $Hc = \frac{\hbar}{e\lambda_{el}^2}$), due to the additional quantum phase introduced by H . Using Eq. (4) with $\mathcal{C} = 0.03$ pF and $\lambda_{el} = 0.2$ nm, the positive $\delta\epsilon'_r(H)$ reported at 100 mK on Fig. 3 can be displayed on Fig. 4. Comparison with the calculations, made for large a/λ_{el} , reveals that both *the sign and the sublinear dependence* $\delta\epsilon'_r(H) \sim H^{0.6 \pm 0.2}$ observed on the data are compatible with disorder effects. Moreover, using the roughly logarithmic decrease of $\langle \delta \ln(\Delta_0(H)) \rangle$ with a/λ_{el} , the experimental data are quantitatively compatible with $a \simeq 5\lambda_{el} \simeq 1$ nm, yielding an elementary dipole $p_0 \simeq 10$ D [20]: this is the

good order of magnitude with respect to the 4 D value drawn from pulse echo experiments [21]. Last, let us note that, once reported on Fig. 4, the 50 mK and 70 mK data lie very close to the 100 mK data, yielding the same $\delta\epsilon'_r(H) \sim H^{0.6\pm 0.2}$ as well as the same order of magnitude for a/λ_{el} : these low T data were not reported on Fig.4 since the expression of C_{TLS} used to derive eq. (4) does not hold precisely below 90 mK.

To summarize, the microscopic model presented here allows to fit quantitatively the data with very reasonable parameters. This is due to the extreme H -sensitivity of tunneling through a *disordered* barrier which yields non negligible effects even for $H \ll H_c$. Indeed, suppressing disorder and taking $a = \lambda_{el} = 0.2$ nm, would lead, by standard tunneling calculations, to $\langle \delta \ln(\Delta_0(H)) \rangle \simeq -(H/H_c)^2 \simeq -10^{-8}$, i.e., to an *undetectable quadratic negative* effect, at odds with experiments.

Despite its success in accounting for our data, a limit of our mechanism is that it yields a monotonous H -behavior of $\delta\epsilon'_r(H)$, i.e., it cannot account for the peaked structure around $H = 0.03$ T reported in [11]. However, even if our scenario is based on disorder effects, it might not contradict the interaction picture used in [11]. Indeed, the disorder explanation lies upon a $\Delta_{0,max}(H)$ effect with a very large $H_c \simeq 10^4$ T while the interaction mechanism involves a $\Delta_{0,min}(H)$ effect with a very small $H_c \simeq 10^{-2}$ T (due to the very large number N of correlated TLS's). In the Fig. 3 of [12], it seems that collective tunneling can be viewed simply as a simultaneous tunneling of N elementary dipoles. If it is so, both mechanisms should

simply add up due to their very different H_c . It is well admitted [11] that averaging problems in the interaction picture demand further progress. It should explain, e.g. why, in [11], $\delta\epsilon'_r(H)$ is peaked around a H_c field *decreasing* when T increases, which *naively* amounts to a counter-intuitive *increase* of N when T increases.

V. CONCLUSION

To summarize, a $\epsilon_r(H)$ dependence was shown in a $a - \text{SiO}_{2+x}\text{C}_y\text{H}_z$ glass for $H \sim 1$ T and $T \leq 0.4$ K. This demanded to decrease the T uncertainty to less than 0.5%: beyond chemical differences between glasses, this might explain why previous studies reported undetectable $\epsilon_r(H)$ effects. At low T , the reported $\epsilon_r(H)$ effects were interpreted assuming that tunneling is affected by some disorder within the elementary tunneling barriers of size $a \simeq 1$ nm. This scenario might simply add up to the interacting one previously proposed.

Acknowledgments

Many thanks to P. Ailloud (CNRS/LPS) and P. Trouslard (CEA/INSTN/LVdG) for samples realisation, and to P. Forget for cryogenic help. Useful discussions with D. Boutard, M. Ocio, M. Rotter, J. Joffrin and J.-Y. Prieur are greatly acknowledged.

-
- [1] R. C. Zeller and R. O. Pohl, Phys. Rev. B **4**, 2029 (1971).
 [2] P. W. Anderson, B. I. Halperin and C. M. Varma, Phil. Mag. **25**, 1 (1972); W.A. Phillips, J. Low Temp. Phys. **7**, 351 (1972).
 [3] H. M. Carruzzo, E. R. Grannan and C. C. Yu, Phys. Rev. B **50**, 6685 (1994).
 [4] M. P. Solf and M. W. Klein, Phys. Rev. B **49**, 12703 (1994).
 [5] A. L. Burin and Y. Kagan, JETP **82**, 159 (1996) [Zh. Eksp. Teor. Fiz. **109**, 299 (1996)].
 [6] A. Wurger, Physica B **263**, 253 (1999).
 [7] S. Kettemann, P. Fulde, and P. Strehlow, Phys. Rev. Lett. **83**, 4325 (1999).
 [8] P. Strehlow, C. Enss, and S. Hunklinger, Phys. Rev. Lett. **80**, 5361 (1998).
 [9] C. C. Yu and A. J. Leggett, Comments Condens. Matter Phys. **14**, 231 (1988).
 [10] P. J. Reijntjes, W. van Rijswijk, G. A. Vermeulen, and G. Frossati, Rev. Sci. Instrum. **57**, 141 (1986); S. A. Wieggers, R. Jochemsen, C. C. Kranenburg, and G. Frossati, *ibid.* **58**, 2274 (1987).
 [11] P. Strehlow *et al.*, Phys. Rev. Lett. **84**, 1938 (2000).
 [12] K-H Ahn and P. Fulde, Phys. Rev. B **62**, R4813 (2000).
 [13] D. Boutard-Gabillet, P. Aranda, F. Ladieu, P. Pari, M. Rotter, J. Non-Cryst. Solids **245**, 27 (1999).
 [14] S. Rogge, D. Natelson, B. Tigner, and D. D. Osheroff, Phys. Rev. B **55**, 11256 (1997).
 [15] If the magnetoresistance of the RuO₂ thermometers were so large to lead to a -6.2 mK shift of the temperature at 50 mK, this would have dramatic consequences in the vast majority of experiments where the H dependence of physical quantities are measured while neglecting the magnetoresistance of the RuO₂: the latter should not lead to corrections over T greater than 5%, contrarily to the 12.4% value corresponding to 6.2 mK for 50 mK.
 [16] In the linear regime, \mathcal{C} is proportionnal to two H -independent parameters of the TLS model: p_0 the elementary TLS dipole, and the density of states.
 [17] P. Hernandez and M. Sanquer, Phys. Rev. Lett. **68**, 1402 (1992); P. Hernandez (1993) Ph.D. Thesis, Paris XI.
 [18] M. Specht, L. P. Levy, F. Ladieu, M. Sanquer, Phys. Rev. Lett. **75**, 3902 (1995).
 [19] E. Medina and M. Kardar, Phys. Rev. B, **46**, 9984, (1992).
 [20] Since $\delta\mathcal{C}_{int.} \propto \eta$, the more general result is $a/\lambda_{el} \simeq 5 + \ln(\eta)$, yielding negligible corrections whatever η in its [0.1, 10] interval.
 [21] G. Baier and M. v. Schickfus, Phys. Rev. B **38**, 9952 (1988).

VI. APPENDIX

A. Proof that η lies in the interval $[0.1; 10]$

It is argued here that, at any reported T , η lies in the interval $[0.1, 10]$. Defining the exponents s and t by $\delta T(1 \text{ T} \leq H \leq 3 \text{ T}) \sim H^t$ and $\delta C_{int.}(1 \text{ T} \leq H \leq 3 \text{ T}) \sim H^s$, we will first assume that $t - s \geq 0.3$ and show, from the data of Fig. 2, that this implies $0.1 \leq \eta \leq 10$ at any reported T . Reciprocally, assuming $0.1 \leq \eta \leq 10$, we will show, by using the trends of Fig. 4 and Fig. 1 that $t - s > 0.3$. Note that s and t are not necessarily integers, due to subtle disorder averaging effects, such as those studied in Medina *et al*'s work [19] (see section IV).

Since we must precisely compare the relative importances in eqs. (1a)-(1b) of the first term containing $\delta T(H)$ and the second one containing $\delta \epsilon_r(H)$, it is more convenient to translate the measured $\delta C(H)$ and the sought $\delta C_{int.}(H)$ into thermal equivalents by introducing $\delta T_C(H) = \delta C(H)/(\frac{\partial C}{\partial T})$ and $\delta T_{int.C}(H) = \delta C_{int.}(H)/(\frac{\partial C}{\partial T})$. Eq. (1a) thus amounts to:

$$\delta T_C(H) = \delta T(H) + \delta T_{int.C}(H), \quad (\text{A1})$$

while defining the corresponding quantities $\delta T_R(H)$ and $\delta T_{int.R}(H)$ for R measurements yields from Eq. (1b):

$$\delta T_R(H) = \delta T(H) + \delta T_{int.R}(H). \quad (\text{A2})$$

With these definitions note that the definition of α given in Eq. (2b) becomes $\alpha = \delta T_{int.R}/\delta T_{int.C}$ with still $\eta = 1/(\alpha - 1)$.

1. Assuming $t - s > 0.3$ implies $0.1 \leq \eta \leq 10$ at any reported T

i) $\eta < 10$ (*i.e.*, $\alpha > 1.1$). Consider the magnitudes of the $\delta C(H)$ and $\delta R(H)$ bumps reported on Fig. 2: for example at 50 mK, these positive bumps around $H = 0.5 \text{ T}$ amount to $\delta T_C \simeq -6 \text{ mK}$ and to $\delta T_R \simeq -7.6 \text{ mK}$. These two values are ten times larger than that derived from the small negative magnetoresistance of the RuO₂ thermometer (see inset of Fig. 1) and, even if the inset data cannot be accurately trusted, these $\delta T_C, \delta T_R$ values are anyway too large to be entirely attributed to the RuO₂ thermometer [15]. This means that both $\delta T_{int.C}(H)$ and $\delta T_{int.R}(H)$ are negative at 50 mK, *i.e.*, $\alpha > 0$ at 50 mK and both $\delta C_{int.}(H)$ and $\delta R_{int.}(H)$ positive in the Tesla range: with the above definition of s , $\delta C_{int.}(H)$ and $\delta R_{int.}(H)$ are expected to be proportionnal to the same H^s with positive coefficients. Thus $\delta C_{int.}(H)$ and

$\delta R_{int.}(H)$ increase with H : the (quasilinear) decrease seen on Fig. 2 at large H thus comes from RuO₂ effects, *i.e.*, $\delta T(H) \propto H^t$ and $t > s$. Setting these H expansions in Eqs. (A1),(A2) leads to $\alpha = (H_R/H_C)^{t-s}$ with H_R the magnetic field where $\delta R(H)$ vanishes and H_C the corresponding one for $\delta C(H)$: at 50 mK, $H_R \simeq 4.2 \text{ T}$ and $H_C \simeq 2.9 \text{ T}$, which with the above assumption $t - s > 0.3$ leads to $\alpha > 1.1$, *i.e.*, $\eta < 10$. Finally, the same argument can be made at $T > 50 \text{ mK}$ where H_R/H_C ratios are larger, reaching 2.5 at 400 mK.

ii) $\eta > 0.1$ (*i.e.*, $\alpha < 10$). The assumption $t > s + 0.3$ implies that the low field region $H \lesssim 1 \text{ T}$ is that where the relative importance of $\delta T_{int.C}$ (*resp.* $\delta T_{int.R}$) in the measured δT_C (*resp.* δT_R) is the largest. In this range where $\delta C(H)$ and $\delta R(H)$ have the same sign, the data of Fig. 2 correspond, for any given T , to values of δT_C and δT_R which differ by less than a factor 2. This means that $\delta T_{int.C}$ and $\delta T_{int.R}$ are of the same order of magnitude (this might be seen also in [11]), hence $\alpha < 10$ *i.e.*, $\eta > 0.1$: this result holds even at large H since α and η do not depend on H .

2. Assuming $0.1 \leq \eta \leq 10$ implies $t - s > 0.3$

This assumption on η allows Fig. 3 and Fig. 4 to be drawn from Fig. 2, yielding $s = 0.6 \pm 0.2$ for $H \gtrsim 1 \text{ T}$. Besides, the data of the lower inset of Fig. 1 about $\theta_{\text{RuO}_2}(H)$ effects amount to $t \gtrsim 1.2$ for $1 \text{ T} \lesssim H \leq 3 \text{ T}$ (note that we do not rely here on the precise values of $\theta_{\text{RuO}_2}(H)$ effects but only on their general trend). Hence, the data ensure $t - s > 0.3$.

B. Ruling out spin effects at low T

Due to the lack of microscopic information on TLS's, spin effects cannot be ruled out at all T . Indeed, if each TLS contains a single electronic spin, the non negligible Zeeman energy $\delta E_Z(H) \simeq 0.7 \text{ K/T}$ comes into play: each TLS becomes a four-level system. This complicates greatly the ϵ_r' calculation in the range $T \gtrsim T_{rev.}$ where the relaxational (*i.e.*, "thermodynamic") contribution plays an important role. This is why the negative $\delta \epsilon_r'(H)$ close to 400 mK has not been interpreted and the efforts were focused on the positive $\delta \epsilon_r'(H)$ at low T . Indeed, well below $T_{rev.}$, the TLS susceptibility is driven by the transitions *coherently* induced by \mathcal{E} , and such quantum transitions are forbidden between states of different spins: TLS's can thus be separated into two *independent* subclasses of a given spin state whose susceptibilities can be added. Thus, for a given spin state, the asymmetry energy Δ between the two potential wells of given TLS is effectively independent of $\delta E_Z(H)$.